Electron impact excitation of H_2O

S. Trajmar,*,† W. Williams,* and A. Kuppermann†
California Institute of Technology, Pasadena, California 91109
(Received 8 August 1972)

Relative differential cross sections for elastic scattering and for a number of inelastic processes corresponding to vibrational and vibronic excitation of H_2O have been determined at 53, 20, and 15 eV impact energies in the 0°–90° angular range. The measurements were carried out with an instrumental resolution of about 80 meV for transitions corresponding to the following energy losses: 0.45 eV (ν_1 and/or ν_3); 0.90 eV ($\nu_1+\nu_3$); 4.5 eV [triplet state(s)]; 7.4 eV ($\tilde{A}\,^1B_1$); 9.7 eV ($\tilde{B}\,^1A_1$); 9.81 eV (triplet state); 10.00 eV [$\tilde{C}\,^1B_1$ (0, 0, 0)]; 10.17 eV [$\tilde{D}\,^1A_1$ (0, 0, 0)]; 10.38 eV [$\tilde{C}\,^1B_1$ (1, 0, 0)]; 10.57 eV [$\tilde{D}\,^1A_1$ (1, 0, 0)]; 10.76 eV [$\tilde{C}\,^1B_1$ (2, 0, 0)] and [$\tilde{D}\,^1A_1$ (1, 1, 0)]; 11.01 eV ($\tilde{E}\,^1B_1$); and 11.11 eV ($\tilde{F}$). On the basis of the angular distribution of the scattered electrons, it is suggested that the 4.5 and 9.81 eV transitions are associated with excitations of triplet states, while the angular distribution of the scattered electrons at all other energy losses indicate predominantly singlet–singlet transitions. The sharpness of the 9.81 eV transition indicates that the corresponding state has an equilibrium geometry similar to that of the ground state.

I. INTRODUCTION

The excitation of a water molecule by electron impact was studied by Schulz[1] up to 15 eV using the trapped electron method. He discovered an energy-loss process with an onset of about 3.4 eV, observed a strong transition at around 7.3 eV, and found a general over-all agreement with optical observations. Threshold electron-impact spectrum of H_2O (and D_2O) was also obtained by the SF_6 trapping technique by Compton *et al.*[2] Their spectrum was very similar to that of Schulz, and the low energy-loss feature was observed with an onset of about 4.4 eV. Raff[3] has observed at about 4 eV energy loss a feature in the spectrum of H_2O at 30 eV kinetic energy. Lassettre and co-workers[4–10] studied the electron impact spectrum of H_2O at low scattering angles and at kinetic energies at and above 100 eV. They observed the two broad transitions at 7.41 eV ($\tilde{X}\,^1A_1 \rightarrow \tilde{A}\,^1B_1$) and 9.7 eV ($\tilde{X}\,^1A_1 \rightarrow \tilde{B}\,^1A_1$) energy losses as well as excitation of the $\tilde{C}\,^1B_1$, $\tilde{D}\,^1A_1$, and other Rydberg states. (See Tables I and II for the summary of the known electronic and vibrational states of H_2O.) Their spectra are in good agreement with ultraviolet absorption spectra.[11–15] The low energy-loss feature was not detected under these conditions. Skerbele, Dillon, and Lassettre[16] also studied the excitation of H_2O at low scattering angles and at kinetic energies between 30 and 60 eV with excellent resolution. Besides the previously observed transitions, they have also detected the very weak scattering corresponding to the low energy-loss feature starting at about 4.4 eV energy loss, an indication for a possible transition at about 6.3 eV, and excitation of the ν_2 (0.198 eV), the ν_1 and/or ν_3 (0.453 and 0.466 eV, unresolved), the ($\nu_2+\nu_3$) (0.661 eV), and the ($\nu_1+\nu_3$) (0.899 eV) vibrations. Recent investigations of Celotta and Kuyatt[17] on H_2O and D_2O at impact energies in the 5–10 eV region and at a scattering angle of 45° show the presence of inelastic scattering in the 4–5 eV energy-loss range. Knoop *et al.*[18] studied the energy-loss spectra of water using a double retarding potential difference technique. With a well depth of 2 eV, they found a broad feature centered at about 4.5 eV energy loss and a strong transition peaked at 7.2 eV. They attribute these transitions to triplet states ($^3A_2$ and $^3B_1$).

Azria and Fiquet-Fayard[19] also studied the trapped electron spectrum of water and concluded that the low energy-loss feature was due to contamination. The conclusions drawn from the present work and from the measurements of Knoop[18b] are contrary to their interpretation.

Other indications for low-lying electronic state(s) of H_2O in the 4–5 eV region come from low-energy electron reflection spectrometry[20,21] and from appearance potentials for neutral molecular fragments of H_2O by electron impact.[22] The only optical observation of a weak absorption at around 4.5 eV was made by Larzul *et al.*[23] using 80 cm of liquid water.

It has been implied or suggested in connection with these observations that the low energy-loss feature is due to the excitation of a low-lying triplet state(s) of H_2O.

The interpretation of a large variety of experimental observations in terms of the energy levels of H_2O has been given by Claydon, Segal and Taylor.[24] The eight low-lying electronic states of the molecule have been assigned in a way that is consistent with experimental optical and electron-impact spectra, with other experimental observations and with their semiempirical INDO calculations.

Theoretical calculations[24–31] have not predicted excited state of H_2O lower than about 6 eV above the ground state (vertical excitation energy), although reasonably good agreement between other calculated and experimentally observed levels were found.

It has been demonstrated earlier[32–37] that at impact energies of about 10–20 eV above threshold the angular distribution of the scattered electrons can be quite reliably utilized to distinguish spin-allowed and spin-

TABLE I. Electronic states of H_2O.

State designation[a]	Electron configuration[a]	Vertical excitation energy (eV)
$\tilde{X}\,^1A_1$	$\cdots(3a_1)^2(1b_1)^2$	0.0
Triplet(s)[b]		~4–6
$\tilde{A}\,^1B_1$, continuum[c]	$\cdots(3a_1)^2(1b_1)(3sa_1)$	7.4
$\tilde{B}\,^1A_1$, continuum[c]	$\cdots(3a_1)(1b_1)^2(3sa_1)$	9.7
Triplet[b]		9.81
$\tilde{C}\,^1B_1(0,0,0)$[c]	$\cdots(3a_1)^2(1b_1)(3pa_1)$	10.00
$\tilde{D}\,^1A_1(0,0,0)$[c]	$\cdots(3a_1)^2(1b_1)(3pb_1)$	10.17
$\tilde{C}\,^1B_1(1,0,0)$[c]	$\cdots(3a_1)^2(1b_1)(3pa_1)$	10.38
$\tilde{D}\,^1A_1(1,0,0)$[c]	$\cdots(3a_1)^2(1b_1)(3pb_1)$	10.57
$\tilde{C}\,^1B_1(2,0,0)$[d]	$\cdots(3a_1)^2(1b_1)(3pa_1)$	10.76
$\tilde{D}\,^1A_1(1,1,0)$[d]	$\cdots(3a_1)^2(1b_1)(3pb_1)$	10.76
$\tilde{E}\,^1B_1$[a]	$\cdots(3a_1)^2(1b_1)(4sa_1)$	11.01
F[a]	$\cdots(3a_1)^2(1b_1)(3d)$	11.11

[a] See Ref. 11 for assignments and notations.
[b] This work.
[c] See Refs. 12 and 13.
[d] See Ref. 8.

forbidden transitions. In a previous article[37] we have reported the detection of a new triplet state of H_2O at 9.81 eV energy and the assignment of the low energy-loss feature to the excitation of low-lying triplet state(s) of H_2O on the basis of the angular distribution of the scattered electrons. In this paper a more detailed discussion of the results as well as relative differential cross sections for elastic scattering, for the excitation of these and several other electronic and pure vibrational states of H_2O are reported at impact energies of 15, 20, and 53 eV and at scattering angles ranging 0°–90°.

II. EXPERIMENTAL

The apparatus and the experimental procedures have been discussed earlier.[38,39] An energy-selected electron beam is scattered off an H_2O vapor target (pressure of about 10^{-3} torr). The scattered signal intensity as a function of energy loss is determined at fixed impact energies (E_0) and scattering angles (θ) by repeatedly scanning the energy-loss spectrum many times with the aid of a 1024 channel scaler until adequate signal-to-noise ratios have been obtained. The energy-loss scale is calibrated either with respect to the elastic peak (zero energy loss) or with respect to the excitation of the $\tilde{D}\,^1A_1$ (0, 0, 0) state (10.17 eV energy loss). Examples of energy-loss spectra are given in Figs. 1–5.

The relative scattering intensities at the different energy losses, with respect either to the elastic or to the ($\tilde{X}\,^1A_1 \rightarrow \tilde{A}\,^1B_1$) scattering intensity (which was measured at 7.4 eV energy loss), were determined from each spectrum. The individual angular dependence of these two scattering intensities was separately measured under instrumental conditions which remained unchanged during the corresponding experiments. The angular dependence of the elastic intensity was measured from 10° to 90°. At scattering angles below 10° this intensity cannot be reliably determined with the present apparatus because of contributions from the direct electron beam and saturation of the counting equipment. The angular distribution of the ($\tilde{X}\,^1A_1 \rightarrow \tilde{A}\,^1B_1$) scattering intensity has been determined down to 0°. The reason for this procedure is that both the elastic and the ($\tilde{X}\,^1A_1 \rightarrow \tilde{A}\,^1B_1$) scattering intensities are large and can be obtained with adequate signal-to-noise ratio in a time short compared to instrumental drift times. The intensities of many of the other transitions are small and long scanning times are required. Figure 6 shows the two intensity curves at 20 eV impact energy corresponding to elastic scattering and to the excitation of the $\tilde{A}\,^1B_1$ state. The curves are averages of many runs done over a period of 2 years and are normalized to the same arbitrary units by matching the over-all shapes. The vertical bars indicate the scatter of the data.

An instrumental resolution of about 0.08 eV (full width of elastic peak at half-maximum) was used to obtain this data. In order to get the relative cross sections for the different electronic systems, one would have to take into account the shapes of the spectral feature and the Franck–Condon factors. Since this can not be done accurately for most of the transitions, it was not attempted in the present work.

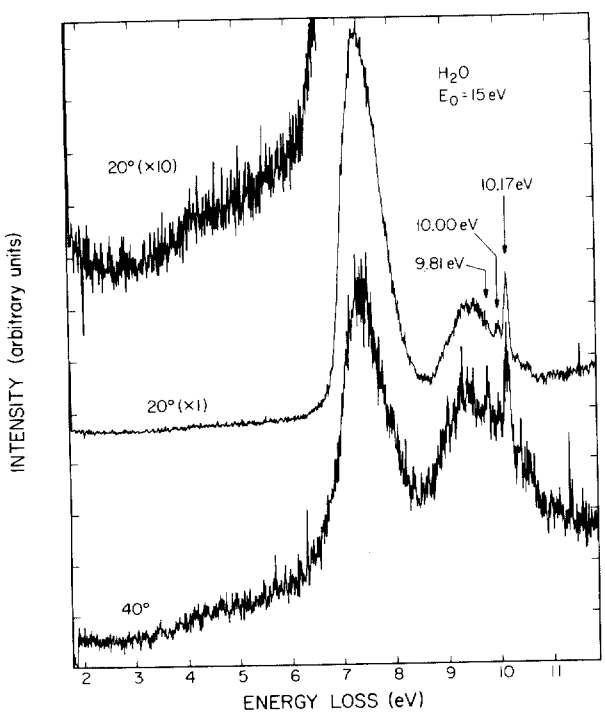

FIG. 1. Energy-loss spectrum of H_2O. $E_0 = 15$ eV, $\theta = 20°$ and 40°. The zero intensity levels for the upper two curves were shifted up to avoid overlapping of the three spectra.

TABLE II. Summary of relative intensities for vibrational excitation.

Upper state	Transition energy (eV)	Intensity: Optical Type[a]	Optical: Penner[f]	Optical: Ferrisso *et al.*[g]	Electron 53 eV, 0°–5° [b]	Impact 15 eV, 60–80° [c]
ν_2	0.198	Ivs	1.00	1.00	1.00	<0.5
$2\nu_2$	0.391	Im	...	...	...	...
ν_1	0.453	Is; Rs	0.72	0.625	0.77	1; 0.77
ν_3	0.466	Ivs				
$3\nu_2$	0.579	...	...	...	...	...
$\nu_1+\nu_2$	0.648	...	...	...	...	...
$\nu_3+\nu_2$	0.661	Im	0.058	0.081	0.046	<0.02
$4\nu_2$	0.762	...	...	...	...	...
$\nu_1+2\nu_2$	0.838	...	...	...		
$\nu_3+2\nu_2$	0.852	Iw	...	...		
$2\nu_1$	0.891	...	...	...		2; 0.080
$\nu_1+\nu_3$	0.899	Im	0.047	0.063	0.034	
$2\nu_3$	0.923	...	...	...		
$5\nu_2$	0.940	...	...	...	...	...
$2\nu_1+\nu_2$	1.084	...	...	...	...	
$\nu_1+\nu_2+\nu_3$	1.092	Is	0.002	...	0.004[d]	<0.005
$2\nu_3+\nu_2$	1.116	...	...	...	...	
$6\nu_2$	1.114	...	...	...	...	...
$2\nu_1+2\nu_2$	1.271	...	...	...	...	
$2\nu_2+\nu_1+\nu_3$	1.300	...	...	...	...	
$2\nu_3+2\nu_2$	1.305	...	...	...	...	3; 0.015
$3\nu_1$	1.313	...	...	...	...	
$2\nu_1+\nu_3$	1.316	Is	...	...	0.003[d]	
$2\nu_3+\nu_1$	1.346	...	...	...	...	
$3\nu_3$	1.403	Im	...	...	...	...
$2\nu_1+3\nu_2$	1.455	...	...	...	...	...
$2\nu_3+3\nu_2$	1.487	...	...	...	...	...
$2\nu_1+\nu_2+\nu_3$	1.506	Im	...	...	...	...
$\nu_2+3\nu_2$	1.558	Ivw	...	...	...	...
$2\nu_1+4\nu_2$	1.634	...	...	...	...	...
$2\nu_3+4\nu_2$	1.670	...	...	...	...	...
$3\nu_1+\nu_3$	1.715	Iw	...	...	...	[e]
$3\nu_3+\nu_1$	1.775	Iw	...	...	...	

[a] I and R refer to infrared and to Raman spectra, respectively. The lower case letters have the following meaning: v, very; s, strong; m, medium; w, weak (see Ref. 11 for further details).

[b] Reference 16.

[c] Present work, normalized to Column 6 for feature 1 (ν_1 and/or ν_3 transition). The first number refers to the identification of the feature in Fig. 4, and the second number to the intensity of the feature.

[d] Calculated from the spectrum given in Ref. 16, Fig. 1. These numbers are very approximate and can be in error by as much as a factor of 2. The enhancement of feature 3 (1.32 eV) in the low-energy, high-angle spectrum, however, is far above the limits of uncertainty.

[e] There is an indication for a feature at 1.74 eV.

[f] S. S. Penner, *Quantitative Molecular Spectroscopy and Gas Emissivities* (Addison-Wesley, Reading, Mass., 1959).

[g] C. C. Ferrisso, C. B. Ludwig, and A. L. Thompson, J. Quant. Spectrosc. Radiat. Transfer **6**, 241 (1966).

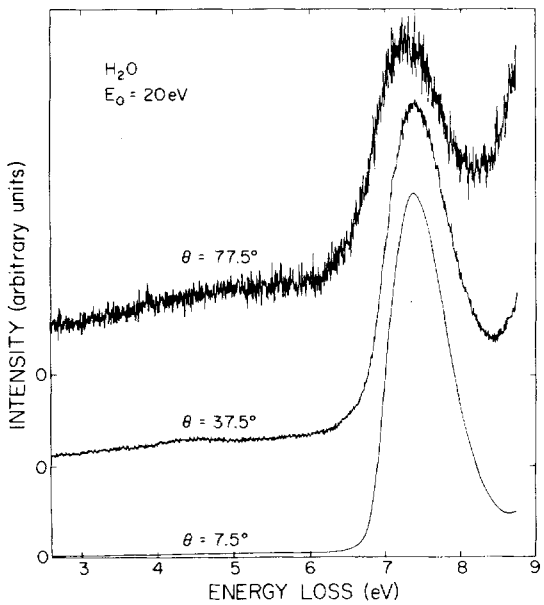

FIG. 2. Energy-loss spectrum of H_2O. $E_0=20$ eV, $\theta=7.5°$, 37.5°, and 77.5°. Zero base line for each spectrum is indicated.

The impact energies were not calibrated in these experiments. In previous experiments on the same apparatus in connection with He, N_2, and O_2, a calibration was carried out using the He 19.31 eV resonance as a reference. It was found that the correction to the impact energy scale varied somewhat with the He to O_2 or He to N_2 ratio but never exceeded 0.050 V. On this basis we believe the impact energy scale is correct to within ± 0.1 eV even for H_2O. In any event the energy-loss scale is independent of this correction and is accurate to about 0.005 eV. The scattering angles are accurate to within $\pm 2°$. The effect of H_2O pressure on the scattered signal intensities was found to be linear from about 0.5 to 2.0 mtorr pressures as measured with an uncalibrated GE miniature ionization guage.

III. RESULTS AND DISCUSSION

A. Energy-Loss Spectra

The known electronic states of H_2O, their vertical excitation energies, and the electronic configurations are listed in Table I. A summary of the vibrational bands of H_2O is given in Table II. Transitions and their intensities as observed in optical and in electron-impact spectra are indicated, and the energies of the other transitions were calculated by using the known vibrational and perturbation constants.[40]

Figure 1 shows the 20° and 40° energy-loss spectra at 15 eV impact energy. At 20° the scattering intensity associated with the features at 4–6 eV and at 9.81 eV are very weak compared to the intensity of the 7.4 eV ($\tilde{A}\ ^1B_1$) excitation. The 20 eV spectra are shown in Figs. 2 and 3. As the scattering angle increases, the relative intensity of these two features with respect to the singlet excitations greatly increases. At 53 eV impact energy and 20° scattering angle the spectrum is shown in Fig. 4. This spectrum is very similar to the 53 eV, 5° spectrum of Skerbele *et al.*[16] with four exceptions: (a) The signal-to-noise ratio in our 20° spectrum is not good enough to show the very weak broad feature in the 4–6 eV energy-loss region; (b) in our spectrum the presence of the 9.81 eV triplet is visible, while in theirs it is not recognizable; (c) the relative intensity of the 7.4 and 9.7 eV features are reversed in the two spectra; (d) the weak shoulder detected by Skerbele *et al.*[16] at 6.2 eV energy loss is not observable in our spectrum.

A typical vibrational excitation spectrum is shown in Fig. 5 at 15 eV impact energy and 80° scattering angle. A complete separation of the individual bands is not possible with the present resolution and an unambiguous assignment cannot therefore be made. One cannot rely fully on optical observations in deciding which transi-

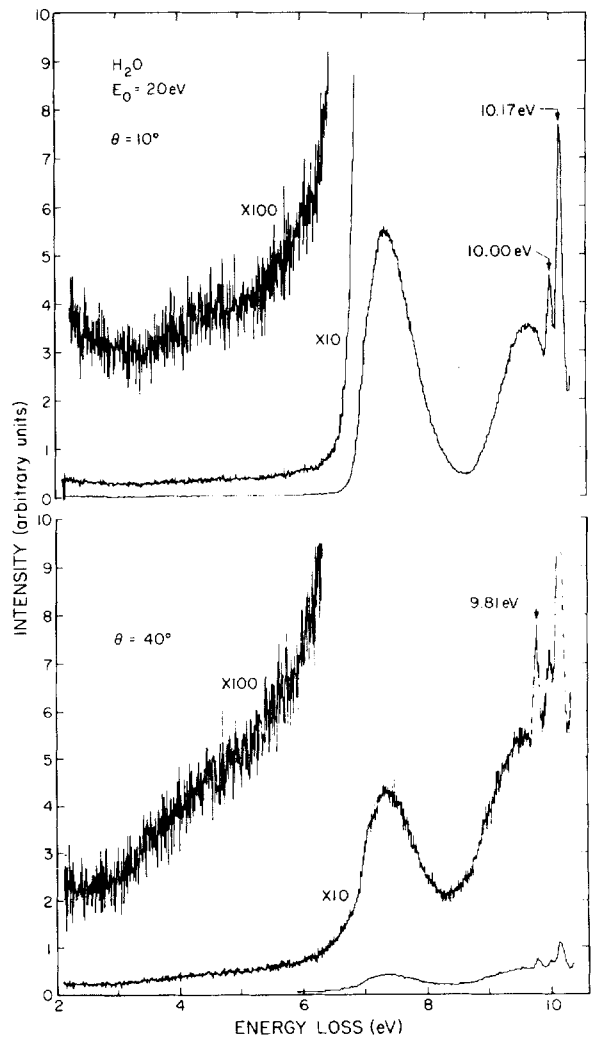

FIG. 3. Energy-loss spectrum of H_2O. $E_0=20$ eV, $\theta=10°$ and 40°. The new 9.81 eV feature becomes very strong at 40°.

tions will be strong and which one will be weak in the electron-impact spectrum. It has been found previously that optically forbidden vibrational bands readily appear in electron-impact spectra.[41–43]

B. Intensity Ratios

Intensity ratios for several electronic transitions with respect to the 7.4 eV transition, as a function of scattering angle, are shown in Figs. 7 and 8 at impact energies of 20 and 53 eV respectively. The ratios have been obtained from the corresponding scattered signal intensities as measured with an instrumental resolution of approximately 0.08 eV at the energy losses indicated for each curve. The observation of a strong feature at around 7.2 eV [1,18] in the threshold spectra of water indicates that the 7.4 eV broad, optically allowed transition can have contribution from this lower lying transition when one deals with the electron impact spectra at low impact energies and high scattering angles. At high impact energies the dominant contribution comes from the $^1B_1$ excitation observed optically at 7.49 eV, while at low energies the contribution is mainly from the triplet excitation at 7.2 eV.[18] In our spectra we observe a gradual shift in the position of the peak from 7.4 eV at 53 eV impact energy to 7.3 eV at 12 eV impact energy. This shift is consistent with a small triplet contribution to this feature. At 20 and 53 eV impact energies, the angular dependence of the DCS for the 7.4 eV energy-loss process (see Sec. III.C and Figs. 12 and 14) is characteristic of an optically allowed transition indicating that at these energies the singlet contribution is dominant. At 15 eV, however, a significant triplet contribution can be present (see Fig. 11).

The electronic transitions are in general broader than 0.08 eV and several of them may overlap; therefore, the intensity ratios and the corresponding DCS's must be interpreted accordingly. Nevertheless, the variation of these ratios with scattering angle at impact energies of about 10–20 eV above threshold can be utilized to distinguish spin-allowed and spin-forbidden transitions as shown by previous work.[32–37] The intensity ratio curves for the spin-forbidden to spin-allowed transitions increase in general by about two orders of magnitude as the scattering angle changes from a few degrees to about 80°. For spin-allowed transitions these ratios are nearly independent of angle.

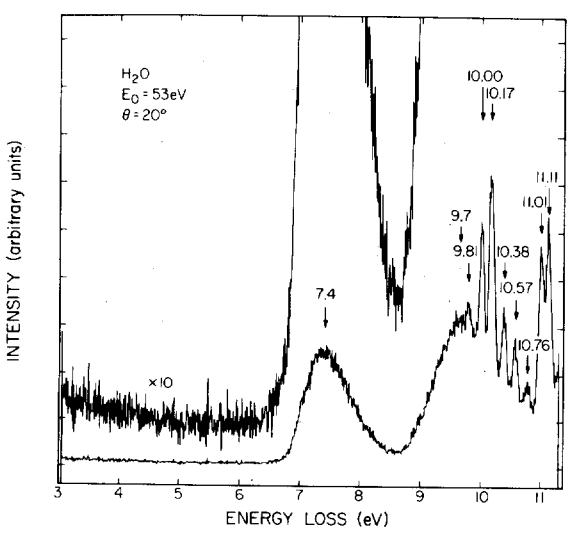

FIG. 4. Energy-loss spectrum of H_2O. $E_0=53$ eV, $\theta=20°$. The energy losses in electron volts are indicated for the spectral features.

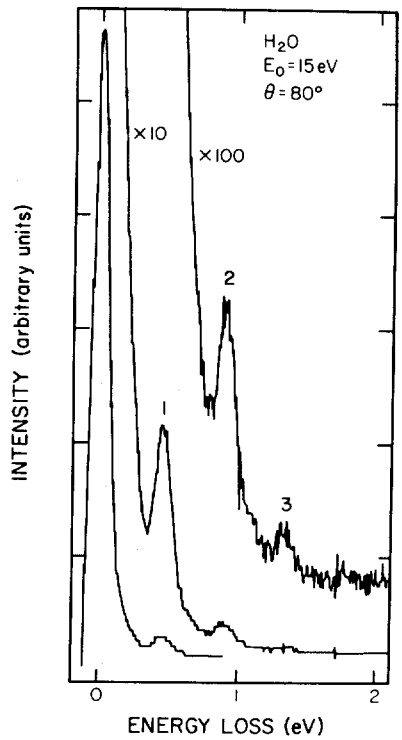

FIG. 5. Vibrational energy-loss spectrum of H_2O. $E_0=15$ eV, $\theta=80°$. See Table II for possible assignment of the features marked as 1, 2, and 3.

Figures 7 and 8 show that at 20 and 53 eV all ratio curves with the exception of those for the 4.5 and 9.81 eV energy losses are very similar and characteristic of spin-allowed transitions. They do not deviate more than about a factor of 2 from their mean value in the 5°–50° angular region. The ratio curve for the 9.81 eV feature changes by more than a factor of about 40 at 53 eV and 100 at 20 eV over this angular range. This is a behavior characteristic of spin-forbidden transitions. The 9.81 eV feature is not resolved in the threshold spectra and is not detectable in the low-angle 53 eV spectrum of Skerbele *et al.*[16] The scattering intensities at 4.5 eV energy loss are very weak, leading to large errors in the corresponding intensity ratios. It can be still deduced, however, that the transition associated with this energy-loss feature has an angular distribution which indicates a spin-forbidden process.

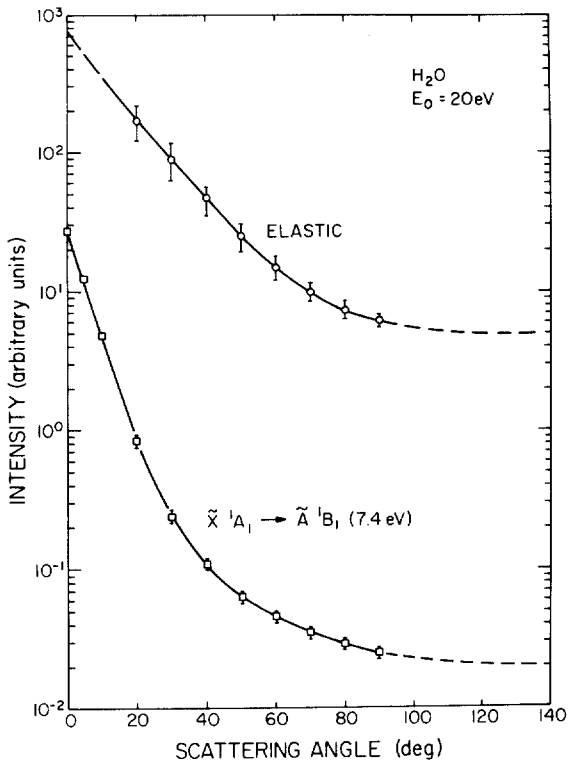

FIG. 6. Scattering intensity (not corrected for "effective path length") as a function of scattering angle for elastic scattering and for excitation of the $\tilde{A}\ ^1B_1$ state at 7.4 eV. The symbols and error bars are the results of several experimental measurements; the solid curve has been drawn through the experimental points, and the dashed part of the curves are extrapolations.

Azria and Fiquet-Fayard[19] studied the energy-loss spectrum of water in the 3–6 eV range. They did not observe the 4.5 eV feature, but when their filament was overheated, a feature at around 3 eV energy loss appeared in their trapped electron spectrum. The intensity ratio for this feature with respect to the 7.4 eV feature decreased as a function of time and also as the pressure in the scattering chamber was increased. On the basis of their observations they concluded that the low energy-loss feature observed in previous investigations[1,2,3,16,18,37] was due to contamination. A comparison of the spectrum obtained by Azria and Fiquet-Fayard with those of the previous investigations clearly shows, however, that their 3 eV feature is not the same as the one observed previously at around 4.5 eV. The nature of this 4.5 eV transition is further discussed in Sec. III.D.

The scattering intensity ratios for vibrational excitations with respect to the elastic scattering are shown in Fig. 9 for 15 eV and in Fig. 10 for 53 eV impact energy. The values reported by Skerbele *et al.*[16] for the same ratio corresponding to the unresolved ν_1 and ν_3 vibrational excitation at 53 eV impact energy are shown as triangles in Fig. 10. The agreement is good except at 15°. If there is a deep minimum in the ratio curve at around 15°, the value reported by Skerbele *et al.*[16] should be more accurate since their angular resolution is about twice as good as for the apparatus used in the present measurements. The ratio curves for the vibrational excitations occurring at 0.45 and 0.90 eV energy losses run parallel to each other at 15 eV impact energy, indicating that the electron impact excitation mechanism is the same for both of them. Similar angular behavior was observed for both homonuclear and heteronuclear diatomic molecules H_2,[31] N_2,[42] and CO [43] at similar impact energies. It seems, therefore, that distinction between opticaly allowed and forbidden transitions in the vibrational spectra will not be possible on the basis of the angular distributions at low impact energies. At 53 eV kinetic energy the relative intensity curve for the combined ν_1 and ν_3 excitations exhibits a dip similar to the one found for the fundamental excitation of H_2 at comparable energies.[41]

C. Differential Cross Sections

The differential cross sections at the indicated energy losses (with an 0.08 eV instrumental resolution) are given in Figs. 11–14.

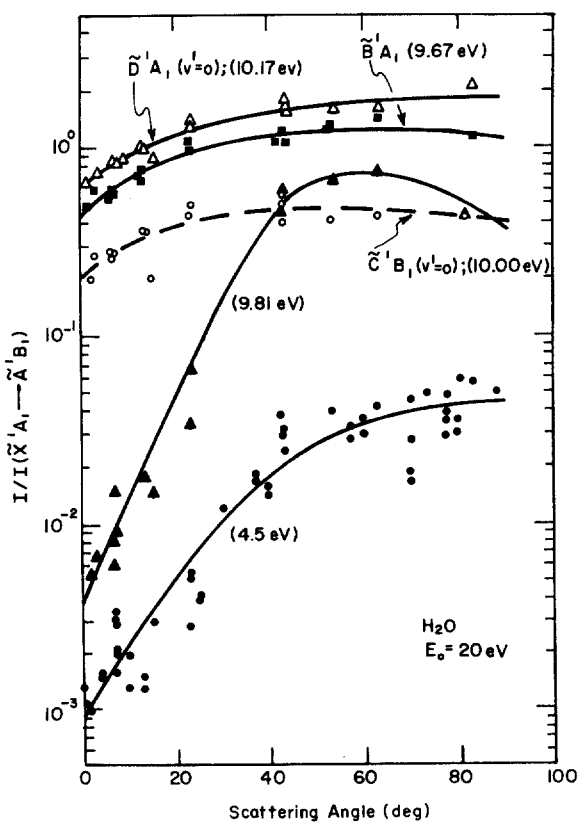

FIG. 7. Scattering intensity ratios of different excitations at the indicated energy losses with respect to the $\tilde{X}\ ^1A_1 \rightarrow \tilde{A}\ ^1B_1$ transition. $E_0 = 20$ eV. The symbols represent the experimental values. The curves have been drawn through the experimental points.

At 15 eV impact energy the elastic and the 7.4 eV DCS's show a fairly strong forward peaking. The DCS's for the different vibrational excitations are nearly isotropic. The 0.90 eV energy-loss feature is probably due to the optically observed strong $(\nu_1+\nu_3)$ band similarly as at higher impact energy[16] but contributions from other bands in that energy-loss region that are weak or absent in the optical spectrum can not be excluded (see Table II). Another weak feature is also observed at 1.32 eV energy loss and shows an angular dependence similar to the 0.45 and 0.90 eV transitions, but it is about an order of magnitude less intense than the 0.90 eV feature.

The DCS curves at 20 eV demonstrate best the characteristic angular distributions for optically spin-allowed, spin-forbidden transitions and for elastic scattering. They can be described as strongly forward peaked, nearly isotropic and intermediate, respectively.

At 53 eV the 9.81 eV transition is well observed at angles greater than about 15°, but only an upper limit can be given at 5° and 10°. The angular behavior of this DCS is distinctly different from all the other ones; it decreases by about a factor of 5 from about 10° to 40°, while the other cross sections decrease by a factor of more than 100. This very strong forward peaking exhibited by all the DCS curves (with the exception of the 9.81 eV transition) is characteristic of optically allowed transitions. Although only the 10.00 and 10.38 eV optical bands have been analyzed as the $\tilde{X}\,{}^1A_1(0,0,0)\rightarrow\tilde{C}\,{}^1B_1(0,0,0)$ and $\tilde{X}\,{}^1A_1(0,0,0)\rightarrow\tilde{C}\,{}^1B_1(1,0,0)$ transitions, respectively,[12,13] all the others have been observed in optical spectra and believed to be Rydberg type of excitations.[11,14,15] The present electron impact results are consistent with these optical results. The elastic DCS is slightly less forward peaked than the DCS for the optically allowed transitions as generally observed in connection with other molecules. The DCS for the vibrational excitation ν_1 and/or ν_3 is quite strongly forward peaked at this impact energy and it is of the same order of magnitude as the DCS's corresponding to the Rydberg transitions. Skerbele *et al.*[16] found that the relative intensities of the vibrational features determined for the electron impact spectrum at 53 eV and low scattering angles were in good agreement with those determined from optical spectra. Table II shows the relative vibrational excitation intensities obtained from optical spectra, from the electron impact spectrum of Skerbele *et al.* at $E_0=53$ eV and $\theta=0°$, and from our electron impact spectrum at $E_0=15$ eV and high scattering angles. The optical and 53 eV electron impact intensities are normalized to unity for the ν_2 band. The 15 eV electron impact intensities were normalized to the combined ν_1 and ν_3 intensities of Skerbele *et al.* It is interesting to note that the relative intensities of the vibrational features at 15 eV impact energy and 80° scattering angle (Fig. 5) are quite different from those at 53 eV and 4° (see Fig. 1 in Ref. 16). The intensity of the ν_2 and $(\nu_2+\nu_3)$ band decreased, while that of the $(\nu_1+\nu_3)$ and $(2\nu_1+\nu_3)$ increased considerably in the 15 eV high-angle spectrum with respect to the 53 eV low-

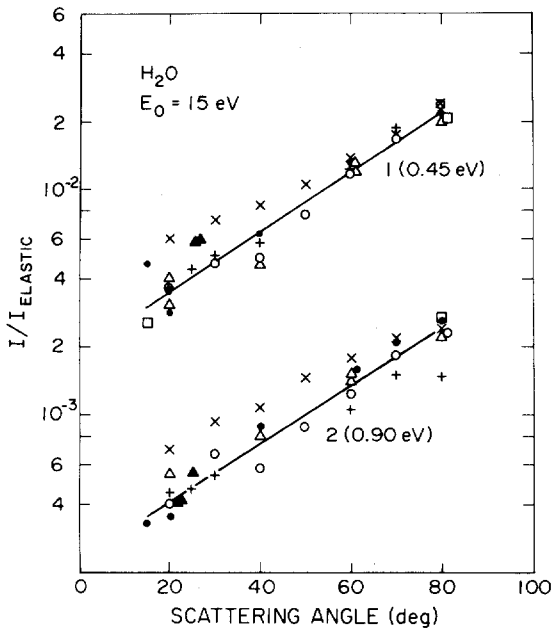

FIG. 9. Scattering intensity ratios with respect to the elastic scattering for the 0.45 and 0.90 eV energy-loss features. The probable vibrational assignments are indicated. $E_0=15$ eV. The symbols represent experimental values. The curves have been drawn through the experimental points.

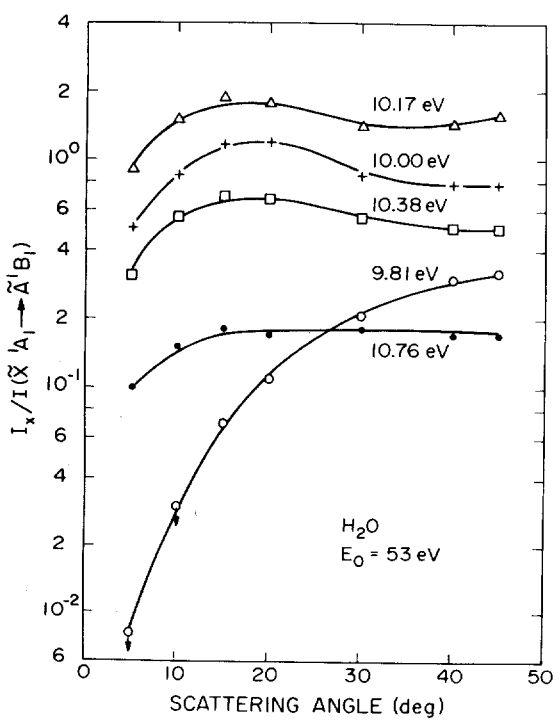

FIG. 8. Same as Fig. 7, except $E_0=53$ eV. The symbols with the arrows represent upper limits.

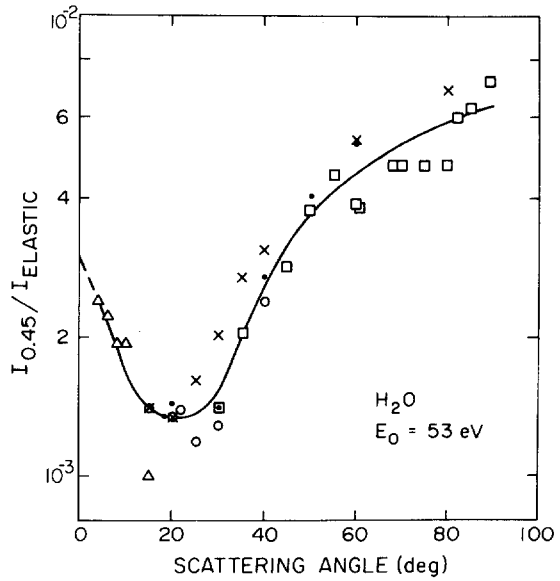

FIG. 10. Same as Fig. 9, except $E_0=53$ eV and the triangles represent the experimental values of Skerbele *et al.* Ref. 16. The other symbols are our experimental results.

angle spectrum. (In both cases the intensities are relative to the 0.45 eV energy-loss feature.) A more accurate evaluation of the energy and angle dependence of the individual vibrational scattering cross sections would require better energy resolution, which in turn would cause the scattering intensities to drop drastically and would make the experiment very difficult or impossible with the present apparatus.

At 20 eV impact energy the integral cross section for the 9.81 eV transition is approximately 85% of the value for the 10.00 eV transition. This same quantity decreases to about 40% at 53 eV impact energy as expected from the triplet nature of the 9.81 eV excitation process.

The relative intensites of the 10.00 and 10.17 eV features also vary with impact energy. $Q_{10.00}/Q_{10.17}$ is 0.25 at 20 eV and 0.53 at 53 eV. The most probable explanation for this change with impact energy is that some triplet excitation process is contributing to the intensity of the 10.17 eV feature.

D. The 4.5 eV Feature

On the basis of the angular distribution of the scattered electrons, the state(s) responsible for the 4.5 eV scattering is classified as a triplet spin state(s). Further indication for this character comes from the energy dependence of the relative intensity of this feature with respect to the ($\tilde{X}\,{}^1A_1 \rightarrow A\,{}^1B_1$) excitation. This ratio is about 0.1 in the trapped electron spectra,[1,2] 0.02 in the spectrum obtained by the double retarding potential difference method at an excess energy of electrons of 2 eV,[18] 0.002 and 0.03 at 10° and 80°, respectively, at $E_0=20$ eV (present work) and 0.001 at a scattering angle of 5° and $E_0=53$ eV.[16] This behavior is consistent with the energy dependence of the cross section ratios of singlet–triplet to singlet–singlet transitions.

As it was pointed out in the Introduction, theoretical calculations do not predict any electronic excited state which would be below 6 eV in the Franck–Condon region of the ground state. On the other hand, a large number of experimental observations indicate excited state(s) at around 4.5 eV. The situation is quite puzzling at the present time and one can only speculate on possible explanations.

The suggestion by Azria and Fiquet-Fayard that the transition is due to a contamination is hard to reconcile with our experimental observations. In the present experiments triply distilled water and a stainless steel sample handling system were used. The same sample handling system with CO gas did not show any scattering in the 3–5 eV energy-loss region under the same conditions as the water spectrum was obtained, indicating that contamination adsorbed on the walls of the sample handling system and the scattering chamber play no obvious role. If the 4.5 eV feature would be associated with a contamination which is present in the H_2O sample, the intensity observations would require a

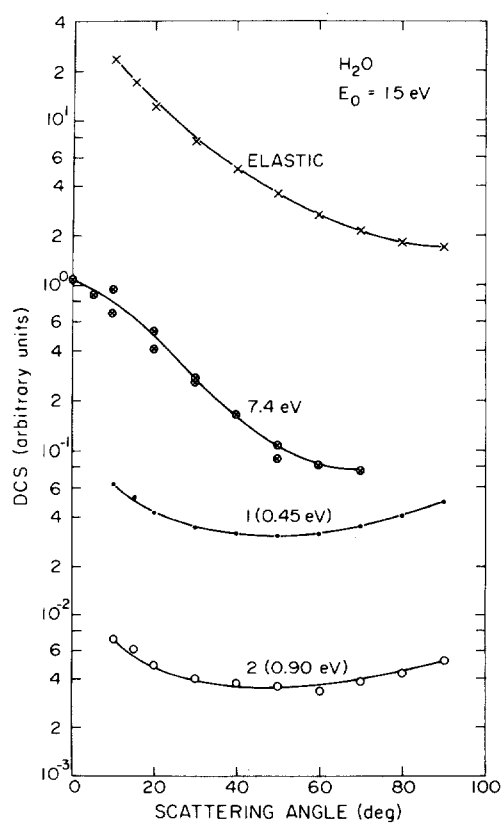

FIG. 11. Differential scattering cross sections for the indicated energy-loss processes. The symbols correspond to experimental results and the curves have been drawn through the experimental points. $E_0=15$ eV.

contamination level of 0.1%–1%. This is clearly unreasonable under our experimental conditions for any contamination. Furthermore, associated with the impurity having a low-lying spin forbidden state at 4.5 eV, one would also expect that other strong optically allowed transitions should show up in the spectrum. Such extra features were not detected. On the basis of these observations we believe that the 4.5 eV energy-loss feature is associated with water and not with a contamination. Knoop[18b] comes to a similar conclusion.

Assuming thermodynamic equilibrium in our scattering chamber, water dimers can not be responsible for this transition since their concentration at room temperature and 1 torr pressure can be estimated from the appropriate equilibrium constant[44] to be more than four orders of magnitude smaller than the monomer concentration. In addition, at the sample pressures and incident electron beam currents used, the steady state concentrations of ionic species are also too small to account for the observed transition intensity.

An explanation in terms of hot bands is not possible. Even if one makes the extreme assumption that the Franck–Condon factors for the hot bands are two orders of magnitude larger than for the normal transition, in order to have the hot band intensity between 1% and 100% of the normal transition intensity at room temperature, it would be required that the hot band energy levels be between 0.24 and 0.12 eV above the ground state. This energy separation is clearly too small

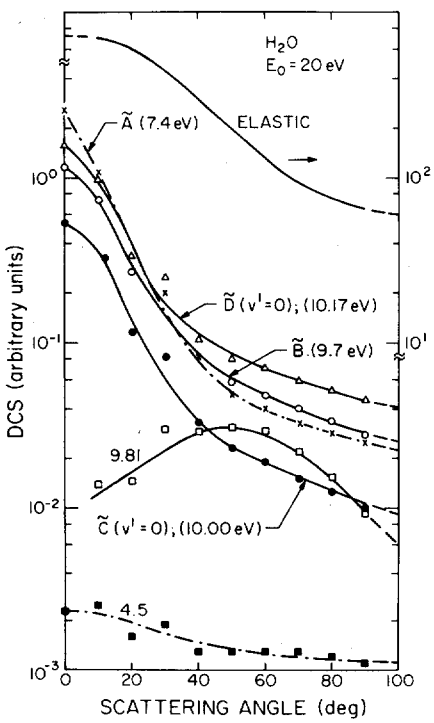

FIG. 12. Same as Fig. 11, except E_0=20 eV and the experimental points for the elastic curve are not shown. The right-hand scale belongs to the elastic curve.

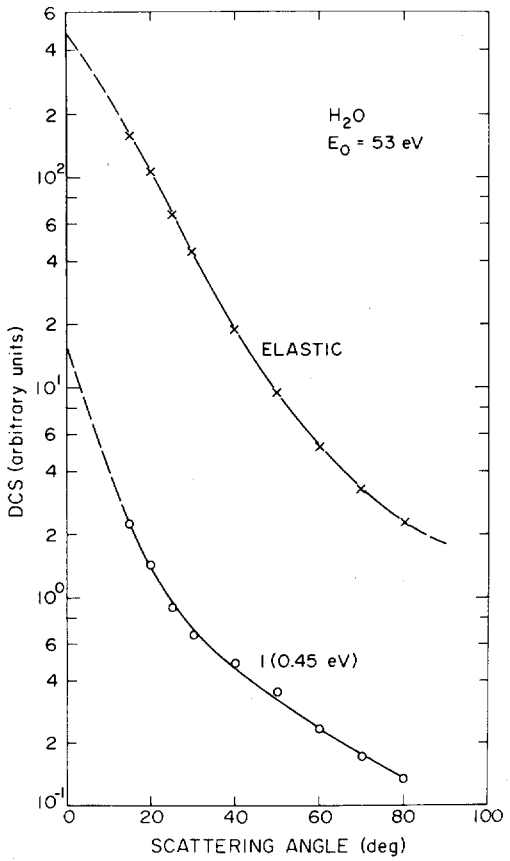

FIG. 13. Same as Fig. 12, except E_0=53 eV.

to explain the difference between the observed transition energies and the calculated ones.

Our observation that the relative intensity of the 4.5 eV transition was approximately the same at 70°C and 9 mtorr as at room temperature and 1 mtorr pressure gives further support for the conclusions drawn in the last two paragraphs.

A possible explanation may be based on the dependence of the ground and excited state energies on the bond bending angle. If at angles different from 104° (which is the equilibrium bond angle for the ground state) the separation of the ground and excited state potential energy surfaces decreases, the low transition energy could be explained. The reason is that for polyatomic potential energy surfaces with different equilibrium geometry, the largest Franck–Condon overlap integral is not necessarily the one which corresponds to a vertical line from the ground state equilibrium geometry to the excited state surface, as in the case for diatomic systems. This does not imply that the nuclei have time to move during the transition, but simply that the maximum in the Franck–Condon integrand of the most probable vibrational band of the electronic transition being considered corresponds to a geometry which differs from the equilibrium geometry of either the ground or excited state and is intermediate

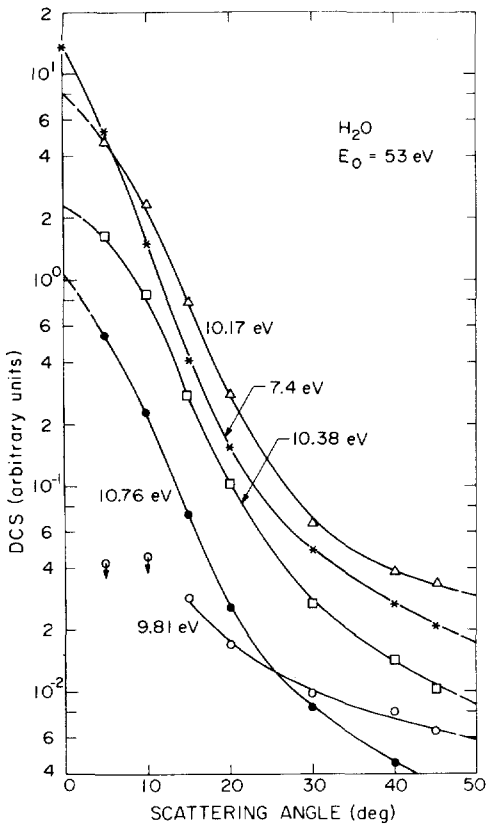

FIG. 14. Same as Fig. 12, except $E_0=53$ eV. The symbols with the arrows represent upper limits.

between both. This would imply that this maximum should be rather weak, in agreement with our measurements. Unrestricted Hartree–Fock calculations of Bader and Gangi[31] for the O atom approaching the H···H pair from a perpendicular direction (corresponding to a C_{2v} geometry) indicate that there are difficulties with this explanation. At the present time we can only say that an accurate calculation of the potential energy surfaces could be very helpful in illuminating this problem.

If we accept the conclusion that the 4.5 eV feature is associated with an electronic state of H_2O, then this state must be stable with respect to dissociation by about 1.5 eV (taking the threshold at 3.5 eV, see e.g., Figs. 1 and 2).

On the basis of the broadness of the 4.5 eV feature, it looks possible that more than one electronic transition may be involved. This suggestion is supported by the mixed angular behavior of the scattering.[37]

E. Importance for the Radiation Chemistry of Water

The cross sections for the direct excitation of the 4.5 and 9.8 eV transitions by electron impact are too low for appreciable concentrations of these states to be found in the radiolysis of water. However, as shown recently by Magee and Huang,[45] the initial population ratio of the triplet and singlet manifolds of excited states formed by electron–ion recombination processes in spurs is appreciable, usually greater than unity. Once a triplet is formed, it can decay by radiation or radiationless transitions to the lowest triplet, which, if the discussion of the previous section is correct, is stable towards dissociation and can therefore have a long lifetime. Under these conditions, reactions of triplets with triplets or with scavengers could be significant. Although no direct experimental evidence for such reactions is yet available, the possibility of their existence should be kept in mind in the interpretation of past and the design of future experiments.

IV. SUMMARY AND CONCLUSIONS

On the basis of the angular distribution of the scattered electrons it is suggested that the dominant contribution to the scattering intensities at 4.5 and 9.81 eV energy losses comes from excitation processes requiring spin exchange. The triplet states associated with these transitions may play an important role in the radiation chemistry of H_2O. Several sharp features have been studied in the 10–12 eV energy-loss region which show typical angular behavior corresponding to singlet–singlet transitions and are believed to correspond to excitations of Rydberg-type states of H_2O. Inelastic scattering corresponding to vibrational excitations was observed; the resolution, however, was not good enough to separate the individual bands and to make an unambiguous assignment possible. The DCS's for the observed vibrational excitations all show the same angular dependence at a given impact energy. At 15 eV impact energy the angular distributions are nearly istropic, but at 53 eV the ν_1 and/or ν_3 DCS is strongly forward peaked and surprisingly large (comparable to electronic transitions). The relative intensities of the vibrational features change significantly as the impact energy is increased from 15 to 53 eV. These observations indicate that energy dependence rather than the angular distribution of the scattered signal intensity will distinguish the different types of vibrational excitations.

* Jet Propulsion Laboratory. Work supported by the National Aeronautics and Space Administration under Contract No. NAS7-100.

† A. A. Noyes Laboratory of Chemical Physics, Division of Chemistry and Chemical Engineering. Contribution No. 4524. Work supported in part by the U.S. Atomic Energy Commission, Rept. Code No. CALT-767P4-89.

[1] G. Schulz, J. Chem. Phys. **33**, 1661 (1960).
[2] R. N. Compton, R. H. Huebner, P. W. Reinhardt, and L. G. Christophorou, J. Chem. Phys. **48**, 901 (1968).
[3] L. M. Raff, Ph.D. thesis; University of Illinois, 1962.
[4] E. N. Lassettre, Radiation Res. Suppl. **1**, 530 (1959).
[5] E. N. Lassettre and S. A. Francis, J. Chem. Phys. **40**, 1208 (1964).
[6] A. Skerbele and E. N. Lassettre, J. Chem. Phys. **42**, 395 (1965).
[7] A. Skerbele, V. D. Meyer, and E. N. Lassettre, J. Chem. Phys. **43**, 817 (1965).
[8] A. Skerbele and E. N. Lassettre, J. Chem. Phys. **44**, 4066 (1966).

[9] E. N. Lassettre, A. Skerbele, M. A. Dillon, and K. J. Ross, J. Chem. Phys. **48,** 5066 (1968).
[10] E. N. Lassettre, Can. J. Chem. **47,** 1733 (1969).
[11] G. Herzberg, *Molecular Spectra and Molecular Structure. III. Electronic Spectra and Electronic Structure of Polyatomic Molecules* (Van Nostrand, Princeton, N.J., 1966).
[12] J. W. C. Jones, Can. J. Phys. **41,** 209 (1963).
[13] S. Bell, J. Mol. Spectr. **16,** 205 (1965).
[14] K. Watanabe and M. Zelikoff, J. Opt. Soc. Am. **43,** 753 (1953).
[15] W. C. Price, J. Chem. Phys. **4,** 147 (1935).
[16] A. Skerbele, M. A. Dillon, and E. N. Lassettre, J. Chem. Phys. **49,** 5042 (1968).
[17] R. Celotta and C. E. Kuyatt (private communication).
[18] (a) F. W. E. Knoop, H. H. Brongersma, and L. J. Oosterhoff, Chem. Phys. Lett. **13,** 20 (1972); (b) F. W. E. Knoop, Ph.D. Thesis, Rijks University, Leiden, The Netherlands, 1972.
[19] R. Azria and F. Fiquet-Fayard, C. R. Acad. Sc. Paris **B273,** 944 (1971).
[20] D. Lewis and W. H. Hamill, J. Chem. Phys. **51,** 456 (1969).
[21] L. M. Hunter, D. Lewis, and W. H. Hamill, J. Chem. Phys. **52,** 1733 (1970).
[22] D. Lewis and W. H. Hamill, J. Chem. Phys. **52,** 6348 (1970).
[23] H. Larzul, F. Gelebart, and A. Johannin-Gilles, C. R. Acad. Sc. Paris **261,** 4701 (1965).
[24] C. R. Claydon, G. A. Segal, and H. S. Taylor, J. Chem. Phys. **54,** 3799 (1971).
[25] S. R. Paglia, J. Chem. Phys. **41,** 1427 (1964).
[26] Y. Harada and J. N. Murrell, Mol. Phys. **14,** 153 (1968).
[27] T. F. Lin and A. B. F. Duncan, J. Chem. Phys. **48,** 866 (1968).
[28] J. A. Horsley and W. H. Fink, J. Chem. Phys. **50,** 750 (1969).
[29] (a) W. J. Hunt and W. A. Goddard III, Chem. Phys. Lett. **3,** 414 (1969); (b) W. J. Hunt, T. H. Dunning, and W. A. Goddard III, Chem. Phys. Lett. **3,** 606 (1969). (c) D. G. Truhlar, "Application of the Configuration Interaction Method and the Random Phase Approximation to the *Ab Initio* Calculation of Electronic Excitation Energies of H_2O," Int. J. Quant. Chem. (to be published).
[30] K. J. Miller, S. R. Mielczarek, and M. Krauss, J. Chem. Phys. **51,** 26 (1969).
[31] (a) R. F. W. Bader and R. A. Gangi, Chem. Phys. Lett. **6,** 312 (1970); (b) R. A. Gangi and R. F. W. Bader, J. Chem. Phys. **55,** 5369 (1971).
[32] S. Trajmar, W. Williams, and A. Kuppermann, J. Chem. Phys. **56,** 3759 (1972).
[33] J. K. Rice, A. Kuppermann, and S. Trajmar, J. Chem. Phys. **48,** 945 (1968).
[34] S. Trajmar, J. K. Rice, P. S. P. Wei, and A. Kuppermann, Chem. Phys. Lett. **1,** 703 (1968).
[35] A. Kuppermann, J. K. Rice, and S. Trajmar, J. Phys. Chem. **72,** 3894 (1968).
[36] S. Trajmar, J. K. Rice, and A. Kuppermann, Adv. Chem. Phys. **18,** 15 (1970).
[37] S. Trajmar, W. Williams, and A. Kuppermann, J. Chem. Phys. **54,** 2274 (1971).
[38] S. Trajmar, D. C. Cartwright, J. K. Rice, R. T. Brinkmann, and A. Kuppermann, J. Chem. Phys. **49,** 5464 (1969).
[39] S. Trajmar, J. K. Rice, and D. G. Truhlar, J. Chem. Phys. **52,** 4502 (1970).
[40] G. Herzberg, *Molecular Spectra and Molecular Structure. II. Infrared and Raman Spectra of Polyatomic Molecules* (Van Nostrand, Princeton, N.J., 1945).
[41] S. Trajmar, D. G. Truhlar, J. K. Rice, and A. Kuppermann, J. Chem. Phys. **52,** 4516 (1970).
[42] S. Trajmar, J. K. Rice, D. G. Truhlar, and R. T. Brinkmann, 21st Gaseous Electron. Conf., Boulder, Colo., 16–18 October 1968, Abstracts, p. 5.
[43] W. Williams and S. Trajmar, Bull. Am. Phys. Soc. **14,** 849 (1969).
[44] J. S. Rowlinson, Trans. Faraday Soc. **45,** 974 (1949).
[45] J. L. Magee and J. J. Huang, J. Phys. Chem. **76,** 3801 (1972).